

# AMPLITUDE AND PHASE ESTIMATOR FOR REAL-TIME BIOMEDICAL SPECTRAL DOPPLER APPLICATIONS

*Stefano Ricci, Riccardo Matera, Alessandro Dallai*

Department of Information Engineering, University of Florence, Firenze, stefano.ricci@unifi.it

## ABSTRACT

In a typical echo-Doppler investigation the moving blood is periodically insonated by the transmitting bursts of ultrasound energy. The echoes, shifted in frequency according to the Doppler effect, are received, coherently demodulated and processed through a spectral estimator. The detected frequency shift can be exploited for blood velocity assessment. The spectral analysis is typically performed by the conventional Fast Fourier Transform (FFT), but, recently, the application of the Amplitude and Phase Estimator (APES) was proved to produce a good quality sonogram based on a reduced number of transmissions. Unfortunately, the much higher calculation effort needed by APES hampers its use in real-time applications. In this work, a fixed point DSP implementation of APES is presented. A spectral estimate – based on 32 transmissions – occurs in less than 120 $\mu$ s. Results obtained on echo-Doppler investigations on a volunteer are presented.

**Index Terms**— APES, DSP implementation, Sonogram, Spectral Doppler, Blood flow.

## 1. INTRODUCTION

In Pulsed Wave (PW) spectral Doppler, the blood flowing in a vessel is insonified along an angled direction through bursts of ultrasound (US) energy. The bursts are transmitted periodically, one every Pulse Repetition Interval (PRI), which typically ranges in 100 $\mu$ s–1ms. The echoes backscattered from erythrocytes moving across a selected region are affected by a frequency shift that, according to the Doppler effect, is related to particles velocity. In a typical echo-Doppler investigation these echoes are received and processed to display the spectrogram [1], widely employed in the diagnostic practice.

The spectrogram is obtained by estimating the Power Spectral Density (PSD) of the demodulated acquired samples [1]. The typical approach for the PSD calculation is the Fast Fourier Transform (FFT) of a windowed segment of input signal. Unfortunately, the frequency resolution required in diagnostic applications is achievable by FFT only when at least 64–128 samples per estimate are processed. These samples are gathered one per PRI, so that up to 0.1 s can be necessary to gain the needed samples. The

temporal resolution of the sonogram is limited and the analysis of rapid transient, e.g. the ones which occurs during the fast blood accelerations in systole, are difficult and inaccurate.

The Amplitude and Phase Estimator (APES) [2], which is typically used in aerospace applications [3], was shown capable of producing good quality spectrograms [4] and spectral profiles [5] based on 31 transmissions only. This approach, if implemented inside an echograph, would produce a 4-fold improvement in the spectrogram temporal resolution. Unfortunately APES requires much more calculations than the FFT, making its real-time employment quite challenging.

In this work we present an implementation of the APES method for the fixed point TMS320C6455 Digital Signal Processor (DSP) [6] (Texas Instruments Inc, Dallas, TX) which is present on-board of the ULA-OP research echograph [7][8], developed by the University of Florence. The method has been studied in Matlab® (The Mathwork Inc, Natick, MA) to identify the critical points and tune the fixed point math dynamics. A suitable tradeoff between calculation complexity and math accuracy was thus achieved. The algorithm has been carefully coded for maximum speed through an optimal exploitation of the 8 parallel units present in the DSP. Sonograms produced by the final algorithm running on the DSP of the ULA-OP scanner have been compared to corresponding sonograms calculated in a double precision APES implementation in Matlab®. Finally, an *in vivo* test on the carotid artery of a volunteer is presented, where the spectrogram calculated through the proposed approach shows no visible differences with respect to the reference.

## 2. APES

### 2.1. Problem formulation

The APES method can be interpreted like a bank of matched filters. Each filter allows a particular frequency of interest to pass while minimizing the total output power. A detailed explanation of APES can be found in [2]; in this section a brief description is reported for reader convenience. Here  $\bar{X}$  and  $\bar{x}$  represent a matrix and a vector, while  $\bar{X}^T$  and  $\bar{X}^H$  represent the transpose and the complex conjugate transpose of  $\bar{X}$ , respectively.

Let  $\tilde{Y}(l)$  be the vector containing the  $N$  demodulated elements  $y_p$  sampled from a given depth in the  $p$ -th PRI with  $p$  ranging between  $l$  and  $l+N-1$ :

$$\tilde{Y}(l) = [y_l, y_{l+1}, \dots, y_{l+N-1}]^T \quad (1)$$

and

$$\bar{Y} = [\tilde{Y}(l), \tilde{Y}(l+1), \dots, \tilde{Y}(l+N+L-1)] \quad (2)$$

Let  $\tilde{E}_N(\varphi)$  be the  $N$ -point Fourier column vector:

$$\tilde{E}_N(\varphi) = [1, e^{j2\pi\cdot\varphi}, \dots, e^{j2\pi\cdot\varphi\cdot n}, \dots, e^{j2\pi\cdot\varphi(N-1)}]^T \quad (3)$$

The echo,  $y_l$ , generated by a scatterer moving with velocity  $v$  toward the transducer, illuminated by a burst of US at frequency  $f_t$  and repeated at PRF=1/PRI rate, can be described by the following model [4]:

$$y_l = A \cdot e^{-j \cdot 2\pi \cdot l \cdot \frac{2\pi f_t}{c \cdot PRF}} = A \cdot e^{-j \cdot 2\pi \cdot l \cdot \varphi} \quad (4)$$

The sample  $y_l$  is gathered after coherent demodulation in the  $l$ -th PRI. The constant  $A$  accounts for the transmission amplitude, the backscattering properties and the constant phase delay related to the distance from the transducer, while  $c$  represents the speed of sound. According to APES, the PSD is obtained in a three-step process. First, assuming that a normalized Doppler frequency  $\varphi$  is present in the signal  $\tilde{Y}(l)$ , the vector  $\tilde{S}(\varphi)$  is calculated by adding  $L$  segments of  $N$  samples each, after compensating for the phase shift introduced by the delays among PRIs:

$$\tilde{S}(\varphi) = \sum_{l=0}^{L-1} \tilde{Y}(l) \cdot e^{j \cdot 2\pi \cdot l \cdot \varphi} \quad (5)$$

In the second step, the  $N$ -by- $N$  autocovariance of the noise, i.e. the signal to be rejected by the filter bank, is estimated:

$$\bar{R}s(\varphi) = \bar{R}\bar{y} - \tilde{S}(\varphi) \cdot \tilde{S}^H(\varphi) \quad (6)$$

where  $\bar{R}\bar{y}$  is the autocovariance of the input signal averaged over  $L$  segments. In the last step, the PSD at normalized frequency  $\varphi$  is finally calculated, for each of the  $M$  desired frequency points:

$$PSD(\varphi) = \left| \frac{1}{L} \left( \frac{\bar{R}s(\varphi)^{-1} \cdot \tilde{E}_N(\varphi)}{\tilde{E}_N^H(\varphi) \cdot \bar{R}s(\varphi)^{-1} \cdot \tilde{E}_N(\varphi)} \right)^H \cdot \tilde{S}(\varphi) \right|^2 \quad (7)$$

## 2.2. Fast Implementation

The direct implementation of (7) is not convenient. As shown in detail in [3] and briefly reported here, several calculations can be saved. The inversion of a matrix  $\bar{R}s(\varphi)$ , which in (7) occurs for each frequency point, can be avoided by applying the matrix inversion lemma:

$$\bar{R}s(\varphi)^{-1} = \bar{R}\bar{y}^{-1} + \frac{\bar{R}\bar{y}^{-1} \tilde{S} \tilde{S}^H \bar{R}\bar{y}^{-1}}{1 - \tilde{S}^H \bar{R}\bar{y}^{-1} \tilde{S}} \quad (8)$$

Moreover, by using (8) in (7) and factorizing  $\bar{R}\bar{y}^{-1}$  as  $\bar{R}\bar{y}^{-1} = \bar{C} \cdot \bar{C}^H$ , after some calculations [3], we obtain:

$$PSD(\varphi) = \left[ \frac{c(\varphi)}{b(\varphi) \cdot [L-d(\varphi)] + |c(\varphi)|^2} \right]^2 \quad (9)$$

where:

$$\begin{aligned} b(\varphi) &= \tilde{E}_N(\varphi) \cdot \tilde{E}_N^H(\varphi) \\ c(\varphi) &= \tilde{E}_N(\varphi) \cdot \tilde{F}b(\varphi) \\ d(\varphi) &= \tilde{F}b(\varphi) \cdot \tilde{E}_N^H(\varphi) \end{aligned} \quad (10)$$

and

$$\begin{aligned} \tilde{F}a(\varphi) &= \tilde{E}_N^H(\varphi) \cdot \bar{C} \\ \tilde{F}b(\varphi) &= \bar{C}^H \cdot \bar{Y} \cdot \tilde{E}_N^*(\varphi) \end{aligned} \quad (11)$$

After the matrix multiplication  $\bar{H} = \bar{C}^H \cdot \bar{Y}$ ,  $\tilde{F}a(\varphi)$  and  $\tilde{F}b(\varphi)$  can be efficiently calculated by  $2N$  FFT, i.e. one for each column of  $\bar{C}$  and  $\bar{H}$ . Thus, according to this approach, APES basically needs a matrix factorization and inversion ( $\bar{C}$ ), a matrix multiplication ( $\bar{H}$ ) and  $2N$  FFT at  $M$  points.

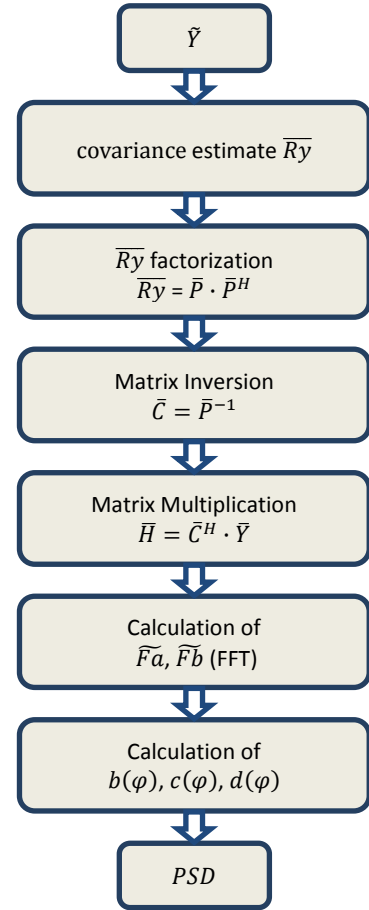


Figure 1. Main calculation steps

## 3. DSP IMPLEMENTATION

The algorithm has been implemented on the fixed point TMS320C6455 DSP [6]. This DSP has a single core of the C64x+™ family, running at 1 GHz. The core is based on the VeliCTI™ very-long-instruction-word (VLIW) architecture and includes 8 parallel calculation units. Up to 2 32x32 bit multiplications (or 4 16x16 bit), 4 summations and 2 32-bit

data transfers to/from the cache memory are possible in a single clock cycle.

The APES method has been coded for  $N = L = 16$ , i.e.  $L+N-1 = 31$  PRIs per estimate, and  $M = 128$  frequency points linearly distributed in the interval 0÷PRF. This choice, according to previous investigations [4][5], represents the optimal balance between frequency resolution and number of PRIs employed per estimate.

According to a preliminary study carried out in Matlab®, the calculations have been implemented in 32-bit fixed point math, with multiplications and accumulations at 64 bit in almost every step. Figure 1 reports the main stages of the procedure. The input vector  $\tilde{Y}$  holds 31 demodulated complex samples represented at 16+16 bit. The algorithm starts estimating the  $16 \times 16$  covariance matrix  $\bar{R}_y$ , which is saved at 32 bit. The Cholesky decomposition is then applied to  $\bar{R}_y$  in order to obtain the lower triangular matrix  $\bar{P}$ , stored at 32 + 32 bit. Since several square roots should be calculated for the decomposition, we have coded a specific Newton-based algorithm for square root estimation adjusted to employ divisions with power of 2 divisors only. In the next step  $\bar{P}$  is inverted. This is a relatively easy task, being  $\bar{P}$  triangular. The result,  $\bar{C}$ , is represented with 32+32 bit.  $\bar{C}$  is then multiplied by the matrix  $\bar{Y}$  composed by segments of the input signal. The 16 columns of  $\bar{C}$  and the 16 columns of  $\bar{H}$  are padded with  $(128-16) = 112$  zeroes. The 32 padded vectors are processed through 128-point FFTs to obtain  $\tilde{F}a$  and  $\tilde{F}b$ , saved at 32+32 bit. An optimized 32+32 bit FFT code distributed by Texas Instruments in the DSPLib<sup>1</sup> was used here. In the last step, the coefficients  $b(\varphi)$ ,  $c(\varphi)$  and  $d(\varphi)$  are calculated at 32+32 bit and the PSD is finally obtained.

## 4. RESULTS

### 4.1. Execution time

TABLE I. EXECUTION TIME

Operation	Clock	Time (μs)
Covariance estimate	$21 \cdot 10^3$	21
Matrix factorization	$22 \cdot 10^3$	22
Matrix inversion	$7 \cdot 10^3$	7
Matrix multiplication	$15 \cdot 10^3$	15
$\tilde{F}a$ and $\tilde{F}b$ calculation (32 FFT)	$34 \cdot 10^3$	34
$b(\varphi)$ , $c(\varphi)$ , $d(\varphi)$ and PSD calculation	$17 \cdot 10^3$	17
<b>PSD calculation on 128 frequency points</b>	<b><math>116 \cdot 10^3</math></b>	<b>116</b>

Thanks to careful code optimization, the most intensive operations are executed with 7 simultaneous operations per clock cycle on average. This leads to the performances listed in Table I. The reported calculation steps have a similar calculation effort, in the order of  $10^4$  clock cycles per step. An overall APES spectrum estimate on 128 frequency points occurs in less than  $12 \cdot 10^4$  clock cycles, corresponding to less than 120 μs when the DSP runs at 1GHz.

### 4.2. Accuracy and sonogram test

The ULA-OP scanner was used to test the proposed implementation. The common carotid artery of a volunteer was investigated with a typical echo-Doppler set-up. The probe was positioned with the help of the B-mode imaging and sonograms displayed in real-time. Several seconds of raw data were saved to be analyzed in post-processing.

In the first test, the accuracy attainable by the proposed DSP implementation has been checked by comparing the spectra calculated by the DSP to reference spectra obtained by processing the same input data in double precision in Matlab®. For example, Figure 2 reports, on top, a typical Doppler spectrum calculated by the DSP and, on bottom, the difference with respect to the reference. The Signal to Noise ratio (S/N), i.e. the ratio between the power of the reference spectra and the power of the error, calculated over more than 3000 spectra, was, on average, S/N = 63 dB.

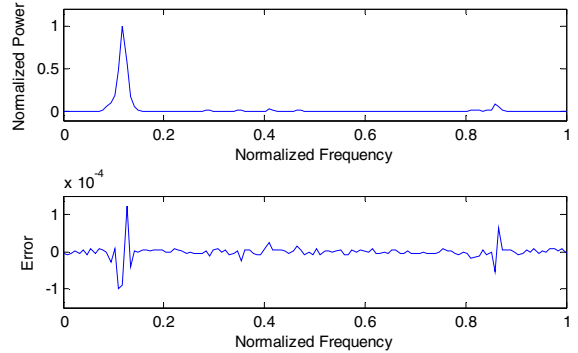


Figure 2. Exemple of power spectrum calculated by DSP (top) and its error with respect to the reference calculated in Matlab (bottom)

In the second test, about 4 s of sonogram have been reconstructed in Matlab® from the saved data through the floating point APES method and compared to the corresponding spectrogram calculated by the DSP. Figure 3 compares the spectrograms calculated by the DSP (top) with the reference (centre). The gray scale covers a 35 dB dynamic range. Both the implementations produce a high-quality spectrogram and no difference is visible between the two over the reproduced dynamic range.

<sup>1</sup> <http://www.ti.com/tool/sprc265>

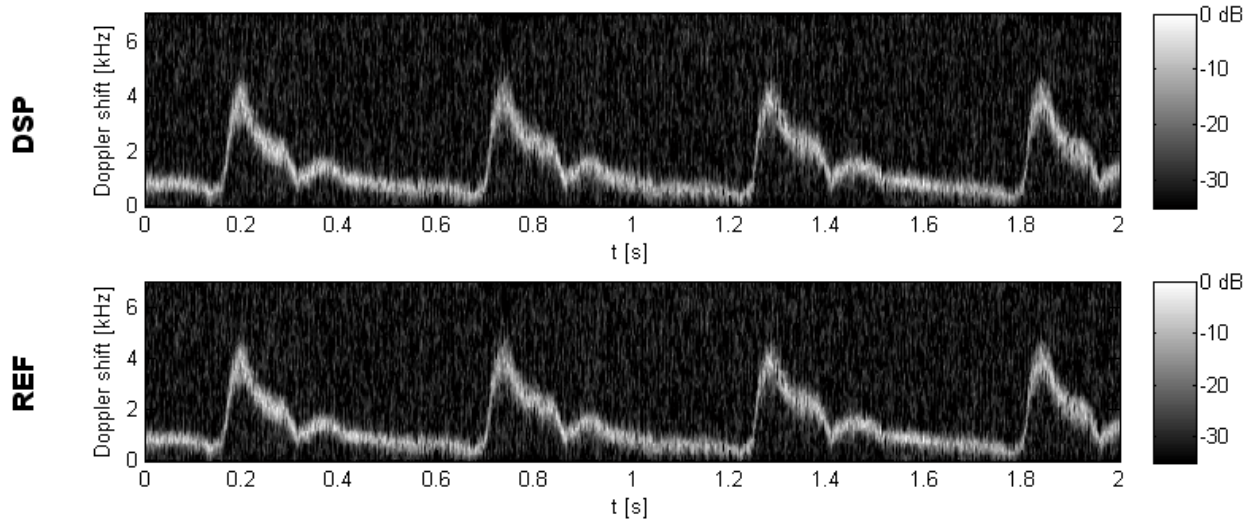


Figure 3. Spectograms obtained by investigating the common carotid artery of a volunteer, calculated by the DSP (top) and Matlab® (bottom).

## 5. CONCLUSION

In this work we presented an APES implementation on the TMS320C6455 fixed point DSP for the real-time elaboration of echo-Doppler biomedical signals. This code can produce a 128-point spectrum estimate in about 120  $\mu$ s, producing a 4-fold improvement on the frame rate with respect to the use of FFT. The elaboration of a spectrogram employs, at 100 fps, about 1% of the DSP calculation power, leaving wide power for concurrent elaborations like B-mode and/or Color Doppler images. The employment of parallel processor can result in further improvement [9].

The implementation features a S/N of 63 dB compared to a reference APES elaboration carried out in double precision. The good performances are confirmed by the comparison reported in Figure 3 where the sonogram calculated by the DSP shows no visible differences with respect to the reference.

The possibility of producing good quality Doppler spectra in real-time, based on a reduced number of PRIs, can be valuable for several applications, like, for example vector Doppler [10] or volume flow assessment [11].

## 6. REFERENCES

- [1] Evans DH, McDicken WN. "Doppler ultrasound Physics, instrumentation and signal processing". Chichester, UK: Wiley, 2000, ISBN: 978-0471970019.
- [2] J. Li and P. Stoica, "An adaptive filtering approach to spectral estimation and SAR imaging.", *IEEE Transactions on Signal Processing*, Vol. 44 No. 6, pp. 1469 - 1484, 1996, <http://dx.doi.org/10.1109/78.506612>.
- [3] Z. S. Liu, L.Hongbin, L. Jian, "Efficient implementation of Capon and APES for spectral estimation", *IEEE Trans. on Aerospace and Electronic Systems*, Vol. 34 No. 4, pp. 1314 – 1319, 1998, <http://dx.doi.org/10.1109/7.722716>.
- [4] F. Gran, A. Jakobsson, J.A. Jensen, "Adaptive Spectral Doppler Estimation", *IEEE Trans. Ultrason., Ferroelect., Freq. Contr.*, vol. 56 no. 4, pp700–713, 2009, <http://dx.doi.org/10.1109/TUFFC.2009.1093>.
- [5] S. Ricci, "Adaptive Spectral Estimators for Fast Flow Profile Detection", *IEEE Trans. Ultrason., Ferroelect., Freq. Contr.*, vol. 60, no. 2, pp. 421-427, 2013, <http://dx.doi.org/10.1109/TUFFC.2013.2579>.
- [6] Texas Instruments, "TMS320C6455 Fixed-Point Digital Signal Processor – Data manual", SPRS276M, <http://www.ti.com/lit/gpn/tms320c6455>.
- [7] P. Tortoli, L. Bassi, E. Boni, A. Dallai, F. Guidi, S. Ricci, "An Advanced Open Platform for Ultrasound Research", *IEEE Trans. Ultrason., Ferroelect., Freq. Contr.*, vol. 56, no. 10, pp. 2207-2216, 2009, <http://dx.doi.org/10.1109/TUFFC.2009.1303>.
- [8] E. Boni, L. Bassi, A. Dallai, F. Guidi, A. Ramalli, S. Ricci, R. Housden, P. Tortoli, "A Reconfigurable and Programmable FPGA based System for non-standard Ultrasound Methods", *IEEE Trans. Ultrason., Ferroelect., Freq. Contr.*, vol. 59 no. 7, pp. 1378-1385, 2012, <http://dx.doi.org/10.1109/TUFFC.2012.2338>.
- [9] D.N. Truong, B.M. Baas, "Massively parallel processor array for mid-/back-end ultrasound signal processing", Biomedical Circuits and Systems Conference (BioCAS) 2010 proceeding, pp. 274 – 277, <http://dx.doi.org/10.1109/BIOCAS.2010.570924>.
- [10] S. Ricci, L. Bassi, P. Tortoli, "Real Time Vector Velocity Imaging through Multigate Doppler and Plane Waves", *IEEE Trans. Ultrason. Ferroelectr. Freq. Control.*, Vol. 62, no. 2, pp. 314-324, 2014, <http://dx.doi.org/10.1109/TUFFC.2014.2911>.
- [11] S. Ricci, M. Cinthio; Å. R. Ahlgren, P.Tortoli, "Accuracy and Reproducibility of a Novel Dynamic Volume Flow Measurement Method", *Ultrasound Med Biol.*, Vol. 39, No. 10, pp. 1903-1914, 2013, <http://dx.doi.org/10.1016/j.ultrasmedbio.2013.04.017>.